	Training	Validation
Number of patients	81	52
Median follow-up (months)	50	26
Number of loco-regional recurrences	28 (35%)	17 (33%)
Treatment	70 Gy concurrent chemotherapy (cisplatin or cetuximab)	
Primary tumor volume (cc)	23.0 (4.0 – 150.8)	29.3 (5.0 – 65.6)
Tumor stage		
T1/T2	33 (41%)	9 (17%)
T3/T4	48 (59%)	43 (83%)
Combined lymph nodes volume (cc)	13.6 (1.0 – 99.1)	8.3 (0.5 – 72.4)
Nodal stage		
N1	11 (14%)	7 (14%)
N2	67 (83%)	43 (83%)
N3	3 (3%)	2 (3%)

Table 1. Studied cohorts of patients. For the volumes of primary tumor and lymph nodes a median and range are given.

Results

The PT model for LRC comprised 3 radiomic features. The mixed model used 4 PT radiomic features (from LC prediction), as a preliminary prediction, combined with 4 LN radiomic features. Both models were significantly associated with LRC in the training and validation cohorts (CI_training_PT = 0.71, CI_validaton_PT = 0.70, CI_training_mixed = 0.80, CI_validaton_mixed = 0.74). The mixed model showed significantly higher performance than the PT model for prediction of LRC ($p < 0.01$). In the combination of PT radiomics and clinical nodal status (TNM) for prediction of LRC, the nodal status was not a significant predictor.

Conclusion

This study shows for the first time that modeling using combined radiomics of the primary tumor and involved lymph nodes improves prediction of the composite endpoint LRC in comparison to primary tumor radiomics only.

PO-0981 Results from the Image Biomarker Standardisation Initiative

A. Zwanenburg[1,2,3,4], M.A. Abdalah[5], A. Apte[6], S. Ashrafinia[7,8], J. Beukinga[9], M. Bogowicz[10], C.V. Dinh[11], M. Götz[12], M. Hatt[13], R.T.H. Leijenaar[14], J. Lenkowicz[15], O. Morin[16], A.U.K. Rao[17], J. Socarras Fernandez[18], M. Vallières[13,19], L.V. Van Dijk[20], J. Van Griethuysen[21], F.H.P. Van Velden[22], P. Whybra[23], E.G.C. Troost[1,2,3,4,24,25], C. Richter[1,2,24], S. Löck[1,2,25]

[1]OncoRay-National Center for Radiation Research in Oncology- Faculty of Medicine and University Hospital Carl Gustav Carus- Technische Universität Dresden- and Helmholtz-Zentrum Dresden-Rossendorf, Dresden, Germany

[2]German Cancer Consortium DKTK, partner site Dresden, Dresden, Germany

[3]German Cancer Research Center DKFZ, Heidelberg, Germany

[4]National Center for Tumor Diseases NCT, partner site Dresden, Dresden, Germany

[5]Moffitt Cancer Center, Department of cancer imaging and metabolism, Tampa FL, USA

[6]Memorial Sloan Kettering Cancer Center, Department of medical physics, New York NY, USA

[7]John Hopkins University, Department of electrical and computer engineering, Baltimore MD, USA

[8]John Hopkins University, Russell H. Morgan department of radiology and radiological science, Baltimore MD, USA

[9]University Medical Center Groningen UMCG- University of Groningen, Department of nuclear medicine and molecular imaging, Groningen, The Netherlands

[10]University Hospital Zurich- University of Zurich, Department of Radiation Oncology, Zurich, Switzerland

[11]The Netherlands Cancer Institute NKI, Imaging technology for radiation therapy group, Amsterdam, The Netherlands

[12]German Cancer Research Center DKFZ, Department of medical image computing, Heidelberg, Germany

[13]LaTIM- INSERM- UMR 1101- IBSAM- UBO- UBL, Brest, France

[14]Maastricht University Medical Centre+, Department of radiation oncology MAASTRO, Maastricht, The Netherlands

[15]Gemelli ART- Università Cattolica del Sacro Cuore, Department of radiation oncology, Rome, Italy

[16]University of California, Department of radiation oncology, San Francisco CA, USA

[17]The University of Texas MD Anderson Cancer Center, Department of bioinformatics and computational biology, Houston TX, USA

[18]Universitätsklinikum Tübingen- Eberhard Karls University Tübingen, Department of radiation oncology, Tübingen, Germany

[19]McGill University, Medical Physics Unit, Montreal, Canada

[20]University Medical Center Groningen UMCG- University of Groningen, Department of radiation oncology, Groningen, The Netherlands

[21]The Netherlands Cancer Institute NKI, Department of radiology, Amsterdam, The Netherlands

[22]Leiden University Medical Center LUMC, Department of radiology, Leiden, The Netherlands

[23]Cardiff University, Cardiff School of Engineering, Cardiff, United Kingdom

[24]Helmholtz-Zentrum Dresden - Rossendorf, Institute of Radiooncology - OncoRay, Dresden, Germany

[25]Faculty of Medicine and University Hospital Carl Gustav Carus- Technische Universität Dresden, Department of Radiotherapy and Radiation Oncology, Dresden, Germany

Purpose or Objective

Radiomics is the high-throughput analysis of medical images for treatment individualisation. It conventionally relies on the quantification of different characteristics of a region of interest (ROI) delineated in the image, such as the mean intensity, volume and textural heterogeneity. The lack of standardisation of image features is one of the major limitations for reproducing and validating radiomic studies, and thus a major hurdle for further developments in the field and for clinical translation. To overcome this challenge, a large international collaboration of 19 teams from 8 countries was initiated to establish an image feature ontology, and to provide definitions of commonly used features, benchmarks for testing feature extraction and image processing software, and reporting guidelines.

Material and Methods

The initiative consisted of two phases. In phase 1, 351 commonly used features were specified and benchmarked against a simple digital phantom, without any requirement for image pre-processing steps. The feature set consisted of commonly used radiomic features and encompasses statistical, morphological and texture characteristics of the ROI, both slice-by-slice (2D) and as a volume (3D). In phase 2, image pre-processing steps were introduced, and features were benchmarked by evaluating five pre-processing configurations on a lung cancer patient CT image. The configurations differ in treatment of the image stack (2D: A-B; 3D: C-E), the interpolation method (none: A; bi/trilinear: B-D, tricubic: E) and the grey-level discretisation method (fixed bin size: A, C; fixed number of bins: B, D-E).

Both phases were iterative, and participants had the opportunity to compare results and update their

workflow implementation. We set the most frequently contributed value of each feature as its benchmark value, and subsequently determined its reliability based on the number of contributing groups and the consensus level.

Results

19 different software implementations were tested. In both phases, only a small number of features were found to be reliable initially. The number of reliable features increased over time as problems were identified and resolved, see Figure 1 and Table 1. Remaining features for which no agreement was reached were not commonly implemented (< 3 agreeing teams), and could therefore not be reliably assessed.

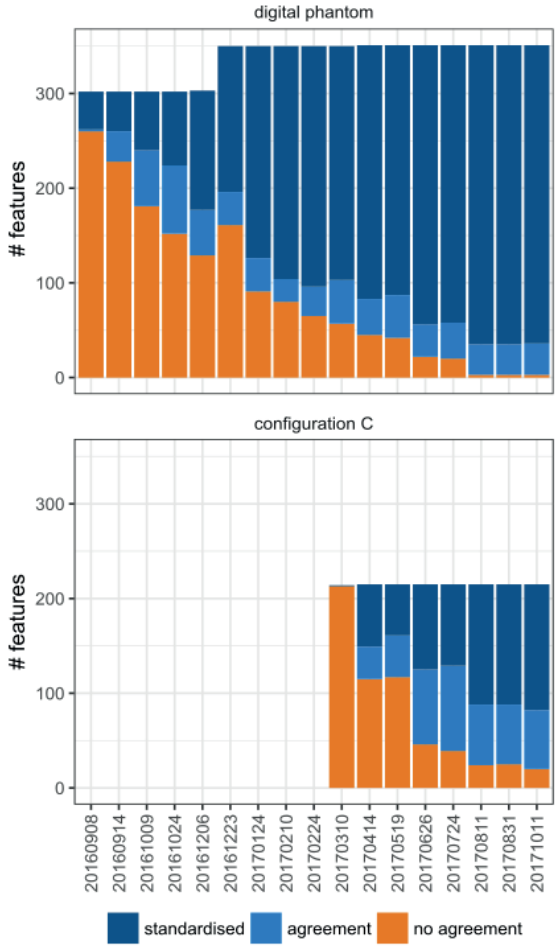

Figure 1: Standardisation progress for the digital phantom (phase 1) and configuration C (phase 2). Reliability is based on consensus *cs* and the number of agreeing implementations *n*: no agreement (*n* < 3 or *cs* < 50%), agreement (50% ≤ *cs* < 80%), and standardised (*cs* ≥ 80%).

	begin phase 1		begin phase 2		last evaluation	
analysis	No	yes	no	yes	no	yes
dig. phantom	86%	14%	16%	84%	1%	99%
configuration A			99%	1%	15%	85%
configuration B			100%	0%	23%	77%
configuration C			99%	1%	9%	91%
configuration D			99%	1%	10%	90%
configuration E			100%	0%	14%	86%

Table 1: Percentage of features for which reliable benchmarks (agreement or standardised) were found at three time points, i.e. start of phase 1, start of phase 2 and the last evaluation.

Conclusion

We addressed the lack of standardised feature definitions, implementation and image pre-processing steps for radiomics by providing reliable benchmark values for commonly used features. During the initiative, the 19 teams demonstrated large initial differences, yet nevertheless managed to converge to common reference values by improving adherence to standardised definitions. Therefore, the use of our standardised definitions and benchmarks to test and update radiomics software is imperative to increase reproducibility of future radiomics studies.

PO-0982 Early MRI biomarkers changes following SRS of brain metastases: correlation with dose

J. Winter[1], F. Ynoe de Moraes[1], C. Chung[2], C. Coolens[1]
[1]*Princess Margaret Cancer Centre, Radiation Medicine Program, Toronto, Canada*
[2]*University of Texas MD Andersen, Department of Radiation Oncology, Houston, USA*

Purpose or Objective

To examine relationships between MRI biomarker changes and dose on a direct voxel-wise basis within GTV of brain metastases and surrounding high dose regions > 12 Gy, a dose level previously linked with radionecrosis. MRI biomarkers included the apparent diffusion coefficient (ADC) computed from diffusion-weighted imaging (DWI), and the contrast transfer coefficient (K_{trans}) and volume of extracellular extravascular space (v_e) extracted from dynamic contrast-enhanced (DCE) MRI. We hypothesized that changes in MRI biomarkers would be related to dose in the early time points following SRS, offering insight into physiological responses to SRS.

Material and Methods

Patients from in house research ethics board approved prospective clinical trials were evaluated. Patients systematically underwent a 3T MRI at day 0, 3 and 20 following SRS as part of their study. The ADC maps were generated by the scanner from DWI. Both K_{trans} and v_e were extracted from DCE-MRI data by fitting the contrast dynamics using the modified Tofts model with a robust 4-D temporal dynamic analysis approach developed in-house. We enabled voxel-wise analyses by developing a rigorous purpose-built image registration pipeline in 3D Slicer and Python to register all MRI biomarker scans to the planning MRI coordinate system, which is linked to both dose and target contours. To assess direct voxel-wise MRI biomarker changes, we computed ΔADC, ΔK_{trans} and Δv_e for day 3 and 20 post-SRS relative to day 0. We performed two analyses. First, we interrogated biomarker differences between days 0, 3 and 20 using the non-parametric Kruskall-Wallice test in the GTV and > 12 Gy non-target region. Second, we performed linear regressions for ΔADC, ΔK_{trans} and Δv_e versus dose within GTV and surrounding > 12 Gy region.

Results

A total of 18 patients (29 brain metastases) were analyzed. Patients received 15 – 21 Gy SRS for a range of primary sites: 2 renal, 7 lung, 2 head and neck, 1 cervix, 4 breast and 2 melanoma. Figure 1 shows the post-contrast T_1 images and biomarker maps for a representative patient. The Kruskall-Wallace test only revealed significant differences for v_e in the GTV between day 0 and 20 ($p < 0.005$) and day 3 and 20 ($p < 0.05$). No significant difference existed in the > 12 Gy region. Linear regressions results showed significant negative correlations with dose for ΔK_{trans} and Δv_e at day 20 within the GTV and > 12 Gy region (Table 1). In contrast, ADC did not exhibit dose-correlated changes except a very weak correlation at day 3 (Table 1).